01 Jan 2003

A Study of the Probe Induced Disturbances on the Near-Field Measurement

Jin Shi

Richard E. DuBroff
Missouri University of Science and Technology, red@mst.edu

Kevin P. Slattery

Masahiro Yamaguchi

et. al. For a complete list of authors, see https://scholarsmine.mst.edu/ele_comeng_facwork/1402

Recommended Citation

J. Shi et al., "A Study of the Probe Induced Disturbances on the Near-Field Measurement," *Proceedings of the IEEE International Symposium on Electromagnetic Compatibility, 2003*, Institute of Electrical and Electronics Engineers (IEEE), Jan 2003.
The definitive version is available at https://doi.org/10.1109/ICSMC2.2003.1428211

A Study of the Probe Induced Disturbances On the Near-Field Measurement

Jin Shi
Electromagnetic Compatibility Laboratory
Department of Electrical and Computer Engineering
University of Missouri-Rolla
Rolla, MO, 65409,U.S.A.
e-mail: shi@umr.edu

Richard E. DuBroff
Electromagnetic Compatibility Laboratory
Department of Electrical and Computer Engineering
University of Missouri-Rolla
Rolla, MO, 65409,U.S.A.
e-mail: red@ece.umr.edu

Kevin Slattery
Intel Desktop Architecture Lab
Hillsboro, OR 97124, USA
e-mail: kevin.p.slattery@intel.com

Masahiro Yamaguchi
Research Institute of Electrical Communication (RIEC)
Tohoku University
Sendai, Japan
e-mail: yamaguti@riec.tohoku.ac.jp

Ken-Ichi Arai
Research Institute of Electrical Communication (RIEC)
Tohoku University
Sendai, Japan

Abstract: Numerical simulations were used to investigate the disturbance introduced by placing a small magnetic loop probe in the near field of a driven loop. In the absence of the loop probe, the numerical simulations were compared with an approximate closed-form analytical expression for the magnetic field produced by the driven loop. The agreement between the approximate analytical results and the simulation was good. The next set of simulations was based on a physical model that included the probe and showed that the probe does exert an effect on the field being measured. Examples of these simulations and their implications on measurements will be discussed.

Keywords: Near field scan, probe disturbance, TLM, FDTD

Introduction

The long-term objective is to use small loop antenna to do near-field scanning and ultimately, we wish to extract the electric and magnetic field emitted by a DUT (Devices Under Test) from the scanning measurements. So it would be helpful for us to know the effect of a loop probe on the near-field measurements. In this paper, numerical simulations were used to investigate the disturbance introduced by placing a small magnetic loop probe in the near field of a driven loop. Firstly, in the absence of the loop probe, the numerical simulations were compared with an approximate closed-form analytical expression for the magnetic field produced by the driven loop. The agreement between the approximate analytical results and the simulation was good. Secondly, a set of simulations was conducted based on a physical model that included the probe. The simulation results showed that the probe does exert an effect on the field being measured. Finally, examples of these simulations and their implications on measurements will be discussed.

Modeling Strategy and Validation

Figure 1 is a photograph of a small square loop fabricated on PCB (printed circuit board) material.

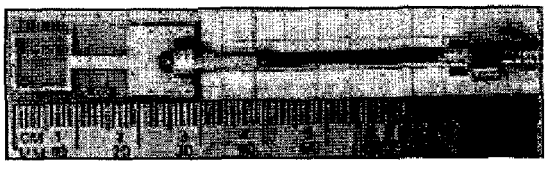

Figure 1. Photography of a square loop probe

The magnetic field produced by this driven loop was calculated using commercial TLM and FDTD programs (specifically FLOEMC® and SEMCAD®). The structure modeled by the TLM and FDTD codes consisted of a square loop having inside dimensions of 8.4 mm by 8.4 mm and outside dimensions of 10 mm by 10 mm. A ground plane was simulated 2 mm below the loop and the values of the magnetic field were calculated at discrete points on a plane located 2 mm above the plane of the loop. These sampling points were uniformly distributed in a two dimensional grid over an area of 21 mm by 21 mm, centered above the center of the driven loop. Figures 2 and 3 show, respectively, the driven square loop and the array of sampling points. Figures 4 and 5 show color plots of the intensities of two magnetic field components— *Hx* and *Hz*, respectively.

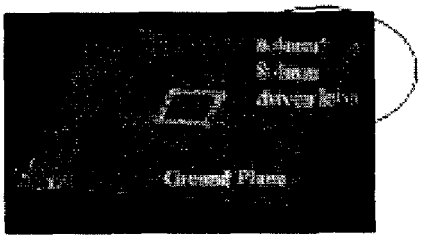

Figure 2. Geometry of the driven loop

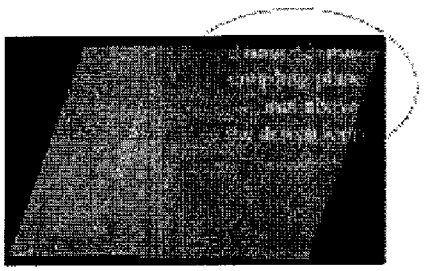

Figure 3. Array of sampling points

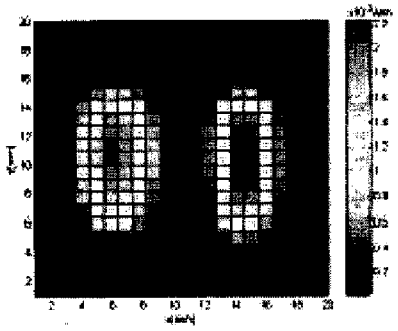

Figure 4. Intensity of *Hx* over array of sample points

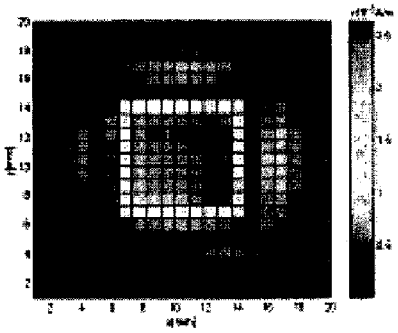

Figure 5. Intensity of *Hz* over array of sample points

These values were obtained numerically from the TLM program and correspond to a frequency of 1 GHz. A closed form quasi-static approximate expression for the magnetic field produced by a planar rectangular loop can be expressed as:

$$\vec{H}(x,y,z) = \hat{x}H_x + \hat{y}H_y + \hat{z}H_z \text{ where}$$

$$H_x = \frac{Ie^{-j\beta R}}{4\pi}\left\{-j\beta\hat{R}(\vec{r}\cdot\hat{z})\ln\frac{(\vec{r}_1+\vec{r}_2+b\hat{y})(\vec{r}_3+\vec{r}_4-b\hat{y})}{(\vec{r}_1+\vec{r}_2-b\hat{y})(\vec{r}_3+\vec{r}_4+b\hat{y})}+\frac{2b(\vec{r}_1+\vec{r}_2)\cdot\hat{z}}{(\vec{r}_1+\vec{r}_4)^2-b^2}+\frac{2b(\vec{r}_3+\vec{r}_2)\cdot\hat{z}}{(\vec{r}_3+\vec{r}_2)^2-b^2}\right\}$$

$$H_y = \frac{Ie^{-j\beta R}}{4\pi}\left\{j\beta\hat{R}(\vec{r}\cdot\hat{z})\ln\frac{(\vec{r}_1+\vec{r}_2+a\hat{x})(\vec{r}_3+\vec{r}_4-a\hat{x})}{(\vec{r}_1+\vec{r}_2-a\hat{x})(\vec{r}_3+\vec{r}_4+a\hat{x})}+\frac{2a(\vec{r}_1+\vec{r}_2)\cdot\hat{z}}{(\vec{r}_1+\vec{r}_2)^2-a^2}-\frac{2a(\vec{r}_3+\vec{r}_2)\cdot\hat{z}}{(\vec{r}_3+\vec{r}_2)^2-a^2}\right\}$$

$$H_z = \frac{Ie^{-j\beta R}}{4\pi}\left\{j\beta\hat{R}(\vec{r}\cdot\hat{x})\ln\frac{(\vec{r}_1+\vec{r}_2+b\hat{y})(\vec{r}_3+\vec{r}_4-b\hat{y})}{(\vec{r}_1+\vec{r}_2-b\hat{y})(\vec{r}_3+\vec{r}_4+b\hat{y})}+\frac{2b(\vec{r}_1+\vec{r}_2)\cdot\hat{x}}{(\vec{r}_1+\vec{r}_4)^2-b^2}-\frac{2b(\vec{r}_3+\vec{r}_2)\cdot\hat{x}}{(\vec{r}_3+\vec{r}_2)^2-b^2}\right.$$
$$\left.-j\beta\hat{R}(\vec{r}\cdot\hat{y})\ln\frac{(\vec{r}_1+\vec{r}_2+a\hat{x})(\vec{r}_3+\vec{r}_4-a\hat{x})}{(\vec{r}_1+\vec{r}_2-a\hat{x})(\vec{r}_3+\vec{r}_4+a\hat{x})}-\frac{2a(\vec{r}_1+\vec{r}_2)\cdot\hat{y}}{(\vec{r}_1+\vec{r}_2)^2-a^2}+\frac{2a(\vec{r}_3+\vec{r}_2)\cdot\hat{y}}{(\vec{r}_3+\vec{r}_2)^2-a^2}\right\} \quad (1)$$

The distances r_1, r_2, r_3 and r_4 are the distances between the field point and the four corners of the loop. The current I is assumed to flow so that the magnetic field in the center of the loop will occur in the $-z$ direction. In the present case, the loop is square so that the distance parameters a and b are equal and simply represent the length of each side of the square loop.

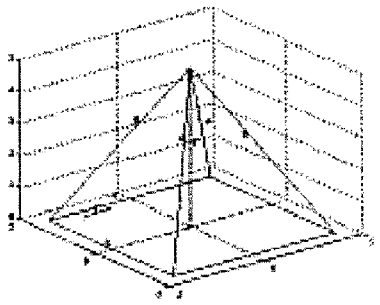

Figure 6. Geometry of a rectangular loop

The corresponding plots of *Hx and Hz* over the same array of sample points are similar to the plots obtained using the TLM method as shown below in Figures 7 and 8.

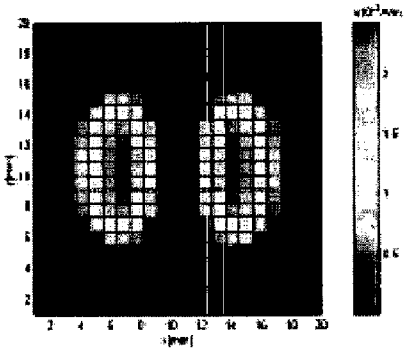

Figure 7. Intensity of *Hx* over array of sample points based on analytic formula

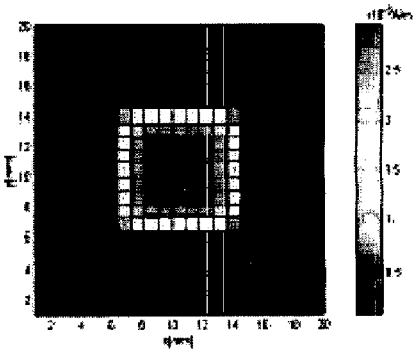

Figure 8. Intensity of *Hz* over array of sample points based on analytic formula

The magnitudes of the magnetic field y-components, while not shown here, are essentially the same as Figures 4 and 7, respectively rotated by 90 degrees. This is not surprising in view of the symmetry of the square loop current distribution.

Probe model and simulation results

The effects of placing a probe in proximity to the driven loop were then modeled using the TLM numerical program. Specifically, a loop probe at the end of a semi-rigid coaxial cable was modeled as shown in the figure below:

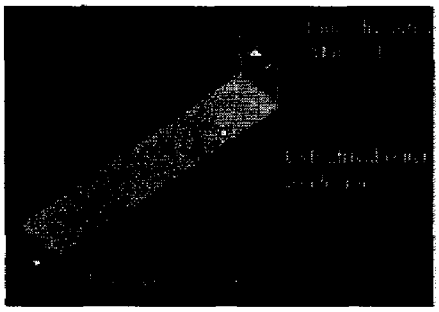

Figure 9. The semi-rigid coaxial loop probe as modeled in the TLM program (relative permittivity =4.22)

The wire connection at the end furthest from the driven loop was modeled as a 50-Ohm resistor. The square cross section of the cable resulted from trying to model the diameter of the semi-rigid cable with only one computational cell in the transverse direction. The simulated probe location was 1.5 mm above the plane of the driven loop with the rectangular cross section of the probe was oriented parallel to the driven loop. The geometric relationship between the cable's cross sectional area and the driven loop are shown below:

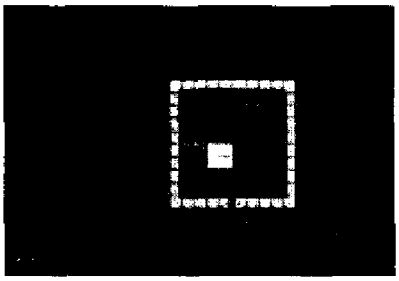

Figure 10(a). The loop of the probe is located 1.5 mm above a point inside the area of the driven loop.

Figure10 (b, c) show two side views of the simulation setup.

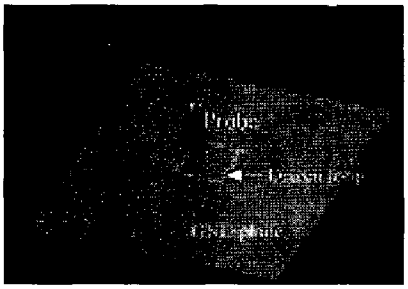

Figure 10(b) Side view of the simulation setup

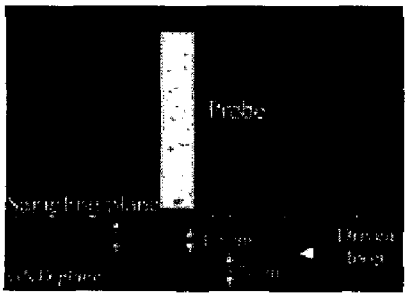

Figure 10(c) Z-X-Axis side view of the simulation setup

The simulations show the magnetic field at all locations in the array of sampling points when the probe location is kept fixed as shown in Figure 10a. The results for the x and z components of the magnetic field are shown in Figures 11 and 12 for the TLM simulation.

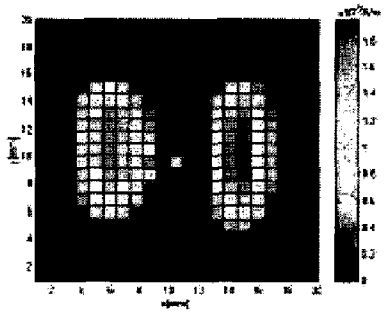

Figure 11. Intensity of *Hx* over array of sample points with probe included (TLM Simulation)

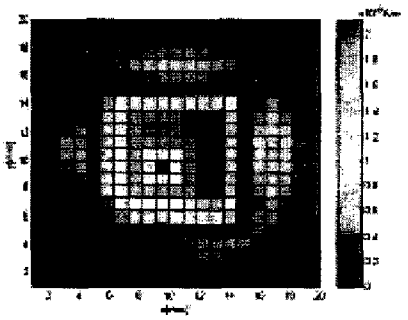

Figure 12. Intensity of *Hz* over array of sample points with probe included (TLM Simulation)

And in Figures 13 and 14 for the FDTD simulation:

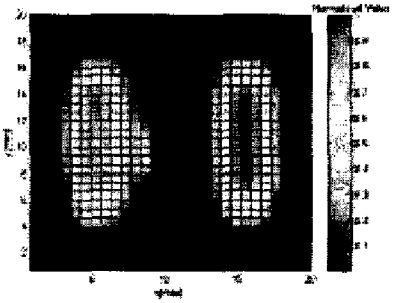

Figure 13. Intensity of *Hx* over array of sample points with probe included (FDTD Simulation)

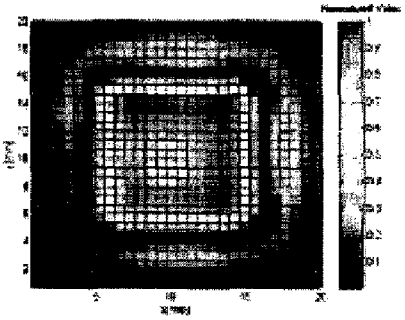

Figure 14. Intensity of *Hz* over array of sample points with probe included (FDTD Simulation)

Data for the y-component was also simulated. The results are not presented here since they essentially consisted of the x-component results rotated by ninety degrees.

Two additional simulations were done to consider the proximity of the probe to the sampling plane and the proximity of the driven loop to the sampling plane and the probe. In Figure 15, the vertical offset between the probe and the driven loop was increased to 5mm while maintaining a 2mm offset between the driven loop and sampling plane. The disturbance in the primary field radiated by the driven loop is apparent in neither the x nor y component shown in Figure 16.

Figure15. Probe position, sampling plane set 5mm and 2.0 mm above the driven loop, respectively

Figure16. Intensity of *Hx* and *Hz* with 5mm between the probe and the driven loop

However if the distance between sampling plane and the probe stays the same, the probe will still introduce disturbance into the near field to be measured. Figure 17 shows the distance between the sampling plane and the driven loop was also increased by 5mm. The simulation results show that the disturbance of the probe still exists.

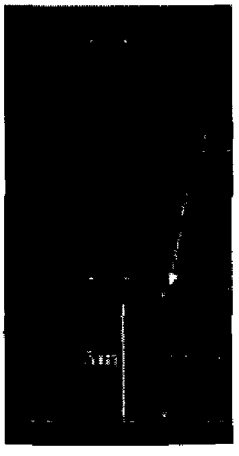

Figure17. Probe position, sampling plane set 5mm , and 5. 5mm above the driven loop, respectively

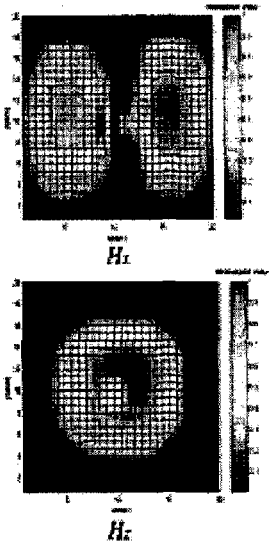

Figure18. Intensity of *Hx* and *Hz* with 5mm between the probe and the driven loop

Conclusion

The presence of a magnetic loop probe can distort near-field measurements. Probe induced distortion may not be harmful in the qualitative characterization of near-zone fields. However the present results suggest that a quantitative characterization of near-zone fields including magnitudes and polarization of near-field components will require some form of probe compensation.

References

[1] T.B.Hansen and A. D. Yaghjian, "Formulation of Probe-Corrected Planar Near-Field Scanning in the Time Domain", *IEEE Trans. Antennas Propagat. , Vol.43, No.6, pp.569-584, 1995*

[2] D.T. Paris, W. M. Leach and E.B. Joy, "Basic Theory of Probe-Compensated Near-Field Measurements ", *IEEE Trans. Antennas Propagat., Vol.AP-26,No.3, pp.373-389 , 1978*

[3] _____ , *FLO/EMC Reference Manual* , Flomerics Incorporated, Southborough ,MA 01772.

[4] _____, *SEMCAD Reference Manual,*, Schmid & Partner Engineering AG, Zurich, Switzerland